Proceedings of GT2007
ASME Turbo Expo 2007: Power for Land, Sea and Air
May 14-17, 2007, Montreal, Canada

GT2007-27967

Laminar Flame Speeds and Strain Sensitivities of Mixtures of H_2 with CO, CO_2 and N_2 at Elevated Temperatures

J. Natarajan, T. Lieuwen, and J. Seitzman
School of Aerospace Engineering
Georgia Institute of Technology
Atlanta, GA 30332-0150

ABSTRACT

Laminar flame speed and strain sensitivities have been measured for mixtures of H_2/CO/CO_2/N_2/O_2 with a wall stagnation flame technique at high preheat temperature (700 K) and lean conditions. The measurements are compared with numerical predictions based on two reaction mechanisms: GRI Mech 3.0 and a H_2/CO mechanism (Davis *et al*.). For H_2:CO 50:50 fuel mixtures, both models tend to over predict the temperature dependence of the flame speed especially at very lean conditions, which confirms the trend found in an earlier study employing a Bunsen flame technique. The predicted strain sensitivities are in good agreement with the measurements. For 50:50 H_2:CO fuel mixtures diluted with 40% CO_2, the amount of over prediction by the models is about the same as in the undiluted case, which suggests that radiation effects associated with CO_2 addition are not important for this mixture at highly preheated lean condition. For low H_2 content (5 to 20%) H_2/CO fuel mixtures at 5 atm and fuel lean condition, the predicted unstrained flame speeds are in excellent agreement with the measurements, but the models fail to predicted the strain sensitivity as the amount of H_2 increases to 20%. Results are also presented for pure H_2 with N_2 diluted air (O_2:N_2 1:9) over a range of equivalence ratios. At lean conditions, the models over predict the measured flame speed by as much as 30%, and the amount of over prediction decreases as the equivalence ratio increases to stoichiometric and rich condition. The measured strain sensitivities are three times higher than the model predictions at lean conditions. More importantly, the predicted strain sensitivities do not change with equivalence ratio for both models, while the measurements reveal a clear trend (decreasing and then increasing) as the fuel-air ratio changes from lean to rich.

[*Keywords:* Syngas, laminar flame speed, reactant preheat, CO_2 dilution, N_2 dilution]

INTRODUCTION

Technologies such as integrated gasification combined cycle (IGCC) plants enable combustion of coal, biomass, and other solid or liquid fuels while still maintaining high conversion efficiencies and low pollution emissions. Synthetic gas (syngas) fuels derived from coal are particularly promising in this regard. Syngas fuels are typically composed primarily of H_2 and CO, and may also contain smaller amounts of N_2, CO_2, H_2O, CH_4, and other higher order hydrocarbons.[1,2].The specific composition depends upon the fuel source and processing technique. This substantial variability in composition, and also heating value, provides a significant barrier to syngas usage. Understanding the impact of this variability on combustor performance or emissions requires an understanding of the fundamental combustion properties of these fuel mixtures. Laminar flame speed is an important parameter of a combustible mixture as it contains fundamental information regarding reactivity, diffusivity, and exothermicity. The value of the flame speed has important impacts upon the propensity of a flame to flashback and blowoff, and also controls other key combustion characteristics, such as flame's spatial distribution. Accurate knowledge of laminar flame speeds is essential for engine design, combustion modeling and validation of kinetic mechanism.

Several prior studies have initiated measurements of the flame speeds of syngas-type mixtures. Laminar burning velocities of syngas mixtures have been measured with Mach Hebra nozzle burners[3] and with Bunsen burners.[4] Laminar flame speeds of H_2/CO mixtures have also been measured with spherically expanding flames[5] and flat flames.[6] However, most of these flame speed measurements are in stoichiometric and fuel-rich mixtures; many low emissions gas-turbine approach require lean premixed combustion. Stretch corrected laminar flame speed measurements for H_2/CO mixtures with counter-

flow flames[7] and spherically expanding flames[8-11] have been obtained and are in fair agreement with each other. However, they cover a limited range of equivalence ratios, relative H_2/CO concentrations, and, most significantly, are restricted to room temperature reactants. Furthermore, most of the measurements are for atmospheric pressures; an exception is the work of Hassan *et al.*[12], who have measured flame speeds at pressures up to 5 atm. Similarly, limited measurements are available for fuels with CO_2 or N_2 dilution. Some measurements and computational studies of CH_4 diluted with CO_2 (to simulate landfill gas) have been reported.[12,13]. Little data on H_2/CO mixtures diluted with CO_2 or N_2 is available.

Recently, the laminar flame speeds of H_2/CO mixtures have been measured over a range of preheat temperature (up to 700 K) and fuel composition.[14] The results indicated that for medium and high H_2 content fuel mixtures, the models over predict the measurements at high preheat temperature and lean conditions. The primary objective of the present study is to measure the strain dependent laminar flame speed and strain sensitivities for medium and high H_2 content syngas fuel mixtures at 700 K preheat temperature and lean conditions with a more accurate, stagnation flame technique. Since most of the syngas mixtures has significant amount of CO_2 and N_2, it is also important to measure the strain dependent laminar flame speed for high amounts of CO_2 and N_2 dilution. The fuel mixtures and test conditions considered in this paper are reported in Table 1. To ascertain the accuracy of current models, the measurements are compared with the predictions of leading models in order to validate them at the high preheat temperatures found in gas turbine combustors.

Fuel (H_2:CO:CO_2)	Oxidizer (O_2:N_2)	Φ	Pressure (atm)	Preheat temperature (K)
50:50:0	21:79	0.6-0.8	1	600-700
30:30:40	21:79	0.6-0.8	1	700
5:95:0-20:80:0	21:79	0.6	5	300
100:0:0	21:79	0.3-0.5	1	700
100:0:0	10:90	0.8-1.6	1	700

Table 1 List of fuel mixtures and test conditions considered for the flame speed measurements.

EXPERIMENTAL FACILITY

Strained laminar flame data were acquired in a stagnation flow configuration. This configuration, like the more common opposed (jet) flow approach,[15] allows for stretch-corrected flame speed measurements of a one-dimensional laminar flame. Furthermore, it is advantageous over the opposed flow arrangement for determining laminar flame speeds for the following reasons: (1) the use of a solid wall leads to more stable flames, (2) problems related to heating of the upper burner are eliminated, and (3) ease of operation of a single jet especially at higher pressures.

A general schematic of the stagnation flow burner is shown in Figure 1. Fuel (H_2, CO, CO_2, and N_2 mixtures) and air flows are monitored with rotameters, and the fuel/air mixture is premixed in the mixing section ahead of the burner. All the rotameters are calibrated with a bubble flow meter and wet test meter to ± 1% accuracy, with fuel and air flows in the range of 0.1 to 50 slpm. The desired flow rate of the premixed fuel mixture is sent to the burner while the remainder is bypassed. With this arrangement, the average velocity of the mixture at the exit of the burner is easily adjusted without altering the equivalence ratio. The burner is formed from a smoothly contoured nozzle with high contraction ratio, in order to create a uniform velocity profile at the burner exit and a uniform flame stretch throughout the flame area. Moreover, the high contraction ratio contoured nozzle ensures laminar flow even at high Reynolds number based on the burner exit diameter.

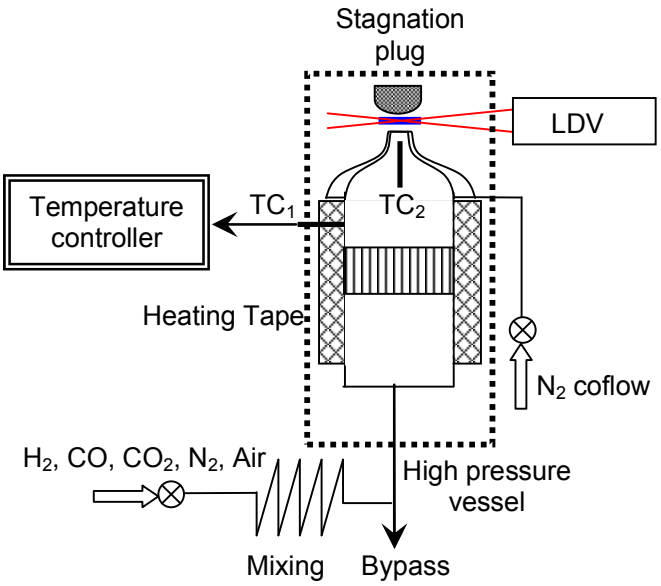

Figure 1 Schematic of the experimental setup (TC=thermocouple). Mixing is achieved through long flow lines.

Various nozzle exit diameters (D=6.25, 9 and 12.5 mm) are employed to produce a stable flame, with higher flame speed mixtures requiring the smaller diameters. Flow straighteners placed upstream of the contoured nozzle reduce any unsteadiness in the incoming flow. The exiting fuel/air mixture is surrounded by a N_2 coflow. Care was taken to reduce the size of the wake region created due to the finite thickness of the contoured nozzle at the burner exit. Flow stagnation is achieved with a plug produced from a stainless steel rod (38 mm diameter). The end of the rod is first formed into a hemisphere and then machined to produce a flat surface with 12.5 mm diameter. The rounded plug, compared to a flat plate, greatly improves flame stability especially at high pressure and high flame speed conditions (e.g., high preheating). The distance (L) between the burner exit and stagnation plug is adjusted depending on the burning velocity. For high burning velocities, a lower L/D leads to a stable stagnation flame. In the

current measurements, L/D ranges from 0.5 to 1. These L/D values are sufficiently large that the effect of finite domain on the measured flame speed can be considered small.[16] The use of a solid wall as a stagnation plane, as opposed to the counterflow configuration with adiabatic twin flames, has insignificant effect on the measured unburned flame speed, provided that the flame is stabilized sufficiently away from the stagnation plane.[17] In all our experiments, the flame is located at least two flame thicknesses away from the plate (and generally more than 5 flame thicknesses). The effects of the solid wall are mainly downstream heat loss from the flame products to the wall and zero radial velocity gradient at the wall. The influence of these effects on the unburned strained flame speed is presented at the end of the results section of this paper for a typical fuel mixture and test condition considered here.

The reactants are preheated by electrical resistance tape wrapped around the burner. Once the desired reactant temperature is achieved (as determined by a type-K thermocouple, TC_2, placed at the center of the burner 25 mm below the exit), the surface temperature of the burner is monitored by a second thermocouple, TC_1, and held constant by a temperature controller. The mixture temperature at the exit of the burner has a nearly uniform radial profile ($\Delta T \approx 3$-5 K). The axial velocity along the stagnation streamline is measured using a Laser Doppler Velocimetry (LDV) system. The fuel mixture is seeded with alumina (Al_2O_3) particles. The nominal size of these particles is chosen to be 1-2 μm in order to minimize thermophoretic effects.[18]

FLAME SPEED MEASUREMENT METHOD

To illustrate this method, the measured axial velocity along the stagnation stream line for a typical stagnation flame is shown in Figure 2. The axial velocity decreases from the exit of the nozzle and reaches a minimum where the preheat zone starts. After reaching a local minimum, the axial velocity increases sharply inside the flame and then decreases to zero at the wall. Based on a common approach, the minimum velocity before the preheat zone is considered as the reference strained unburned flame speed (S_u), and the maximum gradient of the axial velocity before the minimum velocity location is taken as the imposed strain rate (K) (see Figure 2).[15] The imposed strain rate is controlled by changing the nozzle exit velocity. As the nozzle exit velocity increases, the strain rate increases, and the flame moves closer to the stagnation surface. For each fuel mixture, the strain rates and corresponding strained flame speeds are measured for a range of nozzle exit velocities. Effort has been taken to measure the strained flame speeds at as low strain rates as possible, limited either by flashback or flame stability (unsteadiness). The uncertainty in the strained flame speed measurement can be estimated from the rms fluctuation of the axial velocity at the location where the average velocity is a minimum. At each location along the stagnation stream line 10,000 measurements have been taken and the rms fluctuation is less than 3% for all the conditions reported here.

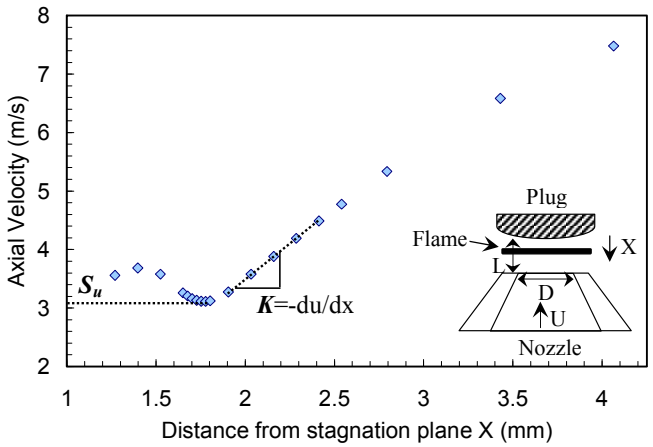

Figure 2 Measured axial velocity along the stagnation streamline for H_2 with N_2 diluted air (O_2:N_2 1:9) mixture at Φ=0.8 and 700 K preheat temperature (D = 9 mm; L = 6 mm). Figure insert shows layout of nozzle generated wall stagnation flame.

FLAME SPEED MODELING

The experimental results are compared to predictions of a standard (Chemkin) one-dimensional flame model. The unstrained laminar flame speeds are calculated with the PREMIX algorithm, while the strained stagnation flames are simulated with OPPDIFF code (but with a premixed reactants). In the strained flame simulation, the distance between the nozzle and stagnation plane (L) was matched to the experimental value, since it can have a significant effect on the predicted strained flame speed. The plug flow boundary condition, which is a close representation of the measured nozzle data, is used at the nozzle exit. The flame speed and strain rate are determined from the stagnation simulation with the same method applied to the experimental data. In all the flame simulations, the converged solution was obtained for a large number of grid points by considering the gradient and curvature to be 0.1. Two reaction mechanisms are employed: GRI Mech 3.0[19] and the H_2/CO mechanism of Davis *et al*.[20] The GRI mechanism has been tested and validated extensively for methane and natural gas combustion over a wide range of pressure and temperature conditions. It consists of 325 elementary chemical reactions with associated rate coefficients and thermochemical properties for the 53 species involved. The second, more recent mechanism was developed specifically for H_2/CO combustion. It consists of 14 species and 30 reactions, and incorporates recent updates for rate parameters and third body efficiencies of a few key reactions. It also includes modifications of thermodynamic and transport properties for species relevant to high temperature H_2 and CO oxidation. In all the simulations, multi-component diffusion and Soret effects (thermal diffusion) have been included, as they have significant influence on the calculated flame speeds, especially for high H_2 content flames.

RESULTS AND DISCUSSION

The prime objective of the present work is to measure the laminar flame speed and strain sensitivity of medium and high H_2 content syngas fuel mixtures at high preheat temperatures and lean conditions. Fuel mixtures of 50:50 H_2:CO were chosen to represent medium H_2 content syngas mixture while pure H_2 has been chosen for high H_2 content mixtures. The validity of the models for high amount of CO_2 and N_2 dilution has been analyzed for medium and high H_2 content fuel mixtures respectively.

Medium H_2 content fuel mixture

An earlier study employing a non-one-dimensional Bunsen flame approach indicated that both GRI Mech 3.0 and the (Davis *et al.*) H_2/CO mechanism tend to over predict the temperature dependence of the flame speed for medium and high H_2 content syngas mixtures at lean conditions.[14] Figure 3 compares the measured flame speed of a 50:50 H_2:CO fuel mixture measured with the Bunsen flame technique with that of the predicted, unstrained, laminar flame speed by both models at two lean equivalence ratios (Φ) and over a range of preheat temperatures. It is clear from this figure that the amount of over prediction by both models increases with preheat temperature. Moreover for a given preheat temperature the over prediction of models increases as the mixture become leaner. For instance, the GRI Mech over prediction increases from 14% at Φ=0.8 to 26% at Φ=0.6 for 700 K preheat temperature. It is also important to note that the H_2/CO mechanism over predictions are larger than for GRI Mech, specifically 16% at Φ=0.8 and 32% at Φ=0.6 and 700K preheat temperature.

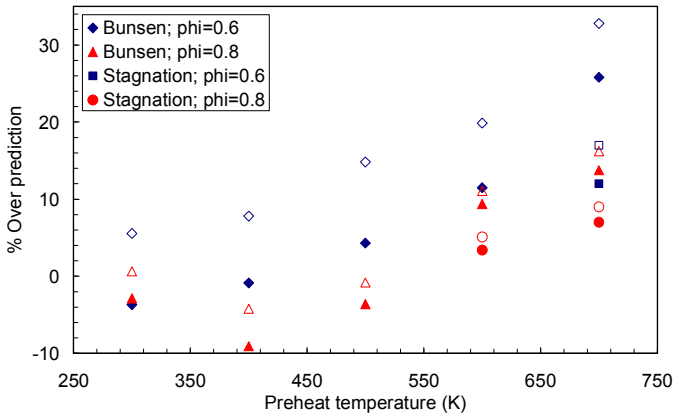

Figure 3 Variation of the models (GRIMech 3.0: Closed symbols; Davis H_2/CO mechansim: Open symbols) over prediction with preheat temperature for 50:50 H_2:CO fuel composition at 0.6 and 0.8 equivalence ratios.

As reported in the earlier study, the Bunsen flame approach to measure the laminar flame speed is based on area weighted average over the entire flame surface.[14] In this method, though the flame is affected by strain and curvature, and these effects are not considered explicitly in the data reduction. Comparing the flame speed measured with the Bunsen flame technique to the unstrained laminar flame speed predicted by the PREMIX algorithm is questionable especially at high preheat temperature where, due to high flame speed and smaller burner diameter, the flame is strongly affected by strain and curvature. The present work focus on measuring the strain dependent laminar flame speed using more accurate stagnation flame technique and compare that to model predictions at high preheat temperatures for medium and high H_2 content syngas fuel mixtures.

Strained laminar flame speeds were measured for the 50:50 H_2:CO fuel composition at an equivalence ratio of 0.8 for a range of strain rates at 600 K preheat temperature (see Figure 4). Due to the very high flame speeds for this mixture and the need for high hydrodynamic strain rate to produce a stable flame, a small nozzle diameter (6.25 mm) with L/D=0.8 was used. The measured flame speed increases linearly as the strain rate increases. The unstrained flame speed (S_u^0) is found by linearly extrapolating the measured strained flame speeds to zero strain rate. The mixture Markstein length (L_M), a measure of the sensitivity of the flame speed to strain, is found from the slope of the linear fit, i.e., $S_u = S_u^0 - L_M \kappa$ as shown in Figure 4. The unstrained flame speed calculated with this approach is 342 cm/s for this condition. Figure 4 also shows the predicted strained flame speeds by both models in the same strain rate range as that of experiment. Again they are linearly dependent on the strain rate, and the unstrained flame speed can be calculated by linear extrapolation. The linearly extrapolated flame speed from the GRI Mech prediction is 328 cm/s, but the unstrained flame speed calculated using PREMIX algorithm with GRI Mech is 306 cm/s for the same condition.

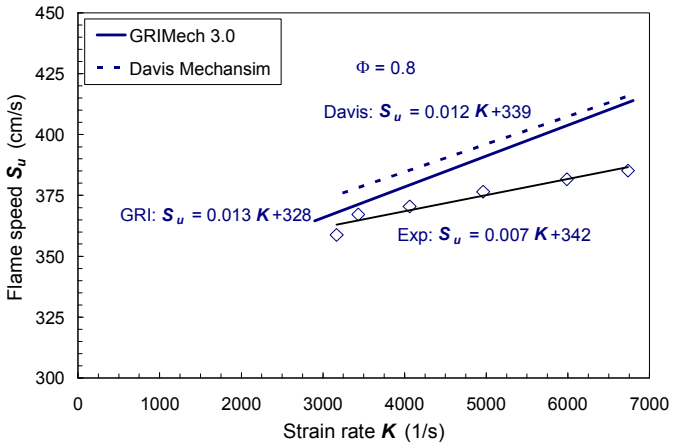

Figure 4 Strained laminar flame speeds for 50:50 H_2:CO fuel composition at 600 K preheat temperature; data (symbols and linear fit) and OPPDIF predictions (lines).

At this point, it should be considered that there may be a significant over prediction of the *unstrained* flame speed in this linearly extrapolation approach mainly due to: (1) the arbitrary definition of the unburned strained flame speed as the minimum velocity point in the approaching velocity profile, and (2) the effect of finite domain. Hence it would be more

appropriate to compare the measured strained flame speed with the corresponding strained flame speed prediction in the same strain rate range. Comparing the strained flame speed in Figure 4, the GRI Mech predictions are in excellent agreement with measurements in the 3000 to 4000 s^{-1} strain rate range but over predict the measurement by 7% in the 6000-7000 s^{-1} range. The H_2/CO mechanism of Davis *et al.* predicts values similar to GRI Mech in the high strain rate range but slightly higher than GRI Mech in the lower strain rate range. For comparison with Bunsen flame approach, a general strain rate has been chosen to be 4000 s^{-1}. At this strain rate, the GRI Mech and Davis mechanism over predict the measurements by 3 and 5% respectively (Figure 3). The Bunsen flame measurement for this condition suggests the GRI Mech and Davis mechanism over predict the measurements by 9 and 11% respectively. Hence, both the measurement techniques consistently show that the models predictions are higher than measurements with the optimized H_2/CO mechanism having slightly larger over prediction for this 50:50 H_2:CO fuel composition at Φ=0.8 and 600 K preheat temperature. Though the predicted strained flame speeds are in good agreement with the measurements, the predicted strain sensitivities are almost twice the measured strain sensitivity (Figure 4).

The strained flame speed for 50:50 H_2:CO mixture at high preheat (700K) was also measured at two equivalence ratios (0.6 and 0.8) where large discrepancies were observed between the Bunsen measurements and model predictions as indicated in Figure 3. A small nozzle diameter (6.25 mm) with L/D=0.8 was used due to high flame speeds for these mixtures.

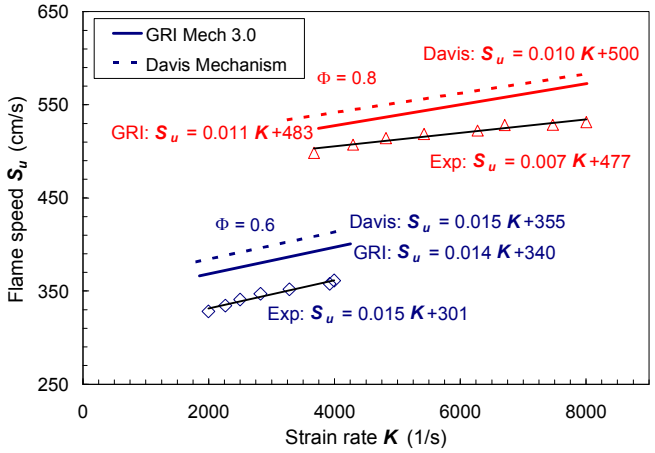

Figure 5 Strained laminar flame speeds for lean mixtures with 50:50 H_2:CO fuel composition at 700 K preheat temperature; data (symbols and linear fit) and OPPDIF predictions (lines).

As seen in Figure 5, the measured strained flame speeds increase linearly with imposed strain rate for both equivalence ratio cases. It is important to note that the flame at Φ=0.6 is more strain sensitive than the Φ=0.8 case. While the predicted and measured strain sensitivities are quite similar, the strained flame speeds predicted with both mechanisms are consistently higher than the measurements for both Φ (see Figure 5). This trend is similar to that found from the Bunsen flame results. The GRI Mech 3.0 calculated strained flame speeds over predict the measurements by 12%, while the Davis *et al*. H_2/CO mechanism over predicts the measurements by 17% for Φ=0.6 over most of the strain rate range. The predictions improve as Φ increases to 0.8, with the GRI results over predicting the measurements by 7%, and the H_2/CO mechanism by 9%. The over prediction of strained flame speed at 700 K is also indicated in Figure 3. As with the Bunsen flame results, the discrepancies between the measurements and model predictions increase as the equivalence ratio decreases for this 50:50 H_2:CO fuel mixture at high preheat temperature. Yet the amount of over prediction with Davis mechanism decreases from approximately 33% in the Bunsen flame case to about 17% for the stagnation flame measurements at Φ=0.6. This could indicate that there is greater discrepancy with the Bunsen flame approach at high preheat temperature due to the increased flame thickness, which leads to a greater uncertainty in locating the true flame surface in order to calculate the flame area accurately.

Effect of CO_2 dilution

The effect of CO_2 dilution at high preheat temperature was studied for this 50:50 H_2:CO composition with 40% CO_2 dilution at lean equivalence ratios. Figure 6 shows the measured strained flame speeds for this composition at 700 K preheat temperature for Φ=0.6 and 0.8. The leaner case has a higher strain sensitivity than that of Φ=0.8 mixture, which is consistent with the undiluted high preheat 50:50 H_2:CO fuel mixture. Figure 6 also shows the predicted strain flame speed by both models for both equivalence ratios.

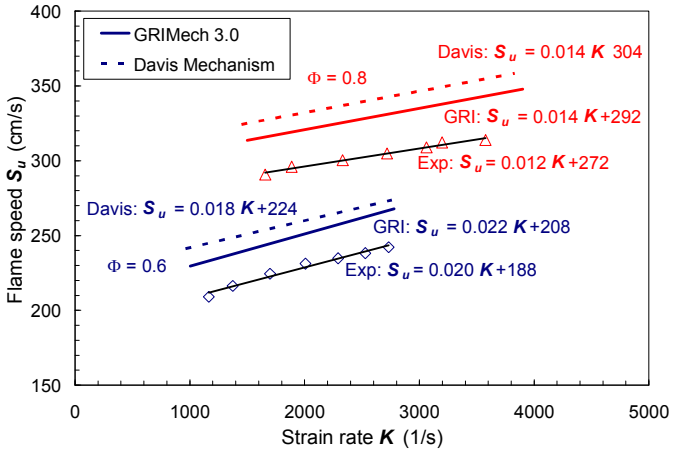

Figure 6 Strained laminar flame speeds for lean mixtures of fuel with 50:50 H_2:CO and 40% CO_2 dilution at 700 K preheat temperatures; data (symbols and linear fits) and OPPDIF predictions (lines).

The predictions with both mechanisms are consistently higher than the measurements and the difference decreases with increasing Φ. In fact, the deviations from the measurements are about the same levels as seen in the undiluted, high preheat

case; the GRI predictions are 10% (Φ=0.6) and 9% (Φ=0.8) above the measurements, while the Davis mechanism results are 14% (Φ=0.6) and 12% (Φ=0.8) too high. This suggests that the radiation absorption/emission effect of CO_2 addition is not important for this mixture even at these highly preheated lean conditions (at least at atmospheric pressure).

Effect of Pressure

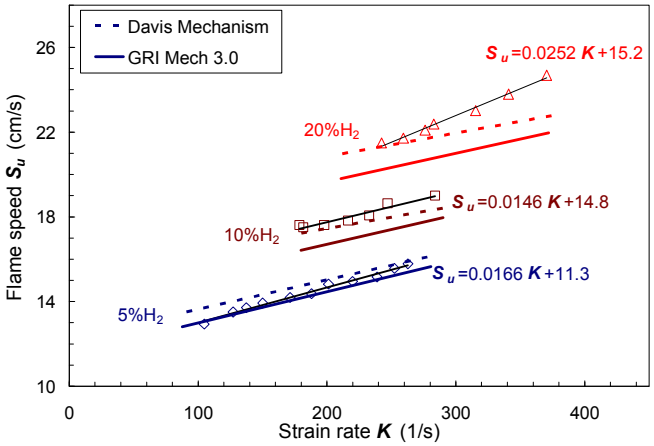

Figure 7 Strained laminar flame speeds for different H_2/CO fuel compositions at 5 atm and Φ=0.6; data (symbols and linear fits) and OPPDIF predictions (lines).

The effect of higher operating pressure at room temperature was studied for three H_2:CO compositions: 5:95, 10:90 and 20:80 at 5 atm and Φ=0.6. The burner diameter used for these measurements is 12.5mm with *L/D* of 0.56. As in the earlier measurements, the flame speed increases linearly with strain rate, indicating a negative (unburned) Markstein length. As the amount of H_2 increases in the mixture, the strain sensitivity increases. For the 5:95 H_2:CO fuel, predicted flame speed by both mechanisms are in excellent agreement (less than 5% discrepancy) with the measurements; this is similar to the finding from the atmospheric pressure tests. Similar agreement between the measurements and predictions is observed for the 10:90 fuel mixture with the H_2/CO mechanism, while the GRI mechanism results slightly under predict the measurements. For both these low H_2 content fuels, the predicted strain sensitivities also are in good agreement with the measurements. Thus the good agreement observed at atmospheric pressure between the model predictions and measurements is maintained at this higher operating pressure. As the amount of H_2 is raised to 20%, the discrepancy between the measurements and predictions increase. The GRI mechanism now under predicts the measurements by about 10%. More importantly both mechanisms fail to predict the higher strain sensitivity for this mixture.

High H_2 content fuel mixture

In order to investigate the validity of the models for high H_2 content syngas mixtures, the strained flame speed has been measured for pure H_2 at 700 K preheat temperature for very lean conditions. The burner diameter used for this fuel mixture is 6.25 mm with *L/D* of 0.8. The measured strained flame speed for various strain rates at Φ=0.3 and 0.5 are shown in Figure 8.

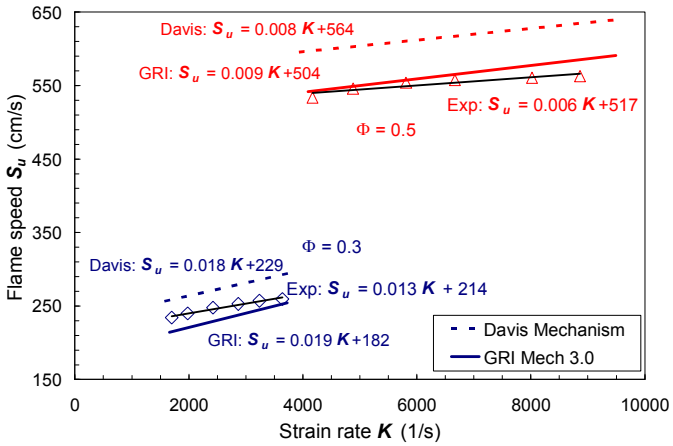

Figure 8 Strained laminar flame speeds for lean mixtures of H_2 at 700 K preheat temperatures; data (symbols and linear fits) and OPPDIF predictions (lines).

The measured flame speed increases linearly with the strain rate for both equivalence ratios, and the leanest case has the higher strain sensitivity. Figure 8 also shows the predicted strained flame speed from both models for both equivalence ratios. For Φ=0.3, the H_2/CO mechanism over predicts the measurement by 10% for all the strain rate range while the GRI Mech predictions are lower than measurements by about 6%. The models predicted strain sensitivities are very similar and they over predict the measured strain sensitivity by about 40%. For Φ=0.5, the GRI mechanism prediction is in excellent agreement with the measured strained flame speed while the H_2/CO mechanism over predicts the measurements by 10%, similar to the Φ=0.3 finding. Again the predicted strain sensitivities are higher than measured strain sensitivity by 40%, similar to the Φ=0.3 case. This result is also similar to the Bunsen flame measurement for high H_2 content syngas mixtures reported earlier, i.e., at high preheat temperature and lean condition the GRI Mech predictions are closer to the measurements than Davis mechanism predictions.

Effect of N_2 dilution

In order to investigate the effect of dilution for this high preheated H_2 fuel mixture, experiments were conducted for pure H_2 fuel with highly N_2 diluted air. The volume ratio of O_2 and N_2 for this N_2 diluted air is 1:9. Due to the high N_2 dilution, the strained flames are very weak and hence it was not possible to get a stable flame at very lean equivalence ratios. The burner diameter used for this fuel mixture is 9 mm with *L/D* of 0.66. Figure 9 shows the measured strained flame speed at Φ=0.8 for a range of strain rates. The measured flame speeds show a nonlinear increase with the imposed strain rate. Though the strained flame speed increases nonlinearly, the unstrained flame speed and strain sensitivity could be calculated by linearly

extrapolating the strained flame speed at lower strain rates (1000-2000 s^{-1}), where it is linear, to zero strain rate. The linear fit of the measurements in this lower strain rate range is also shown in Figure 9.

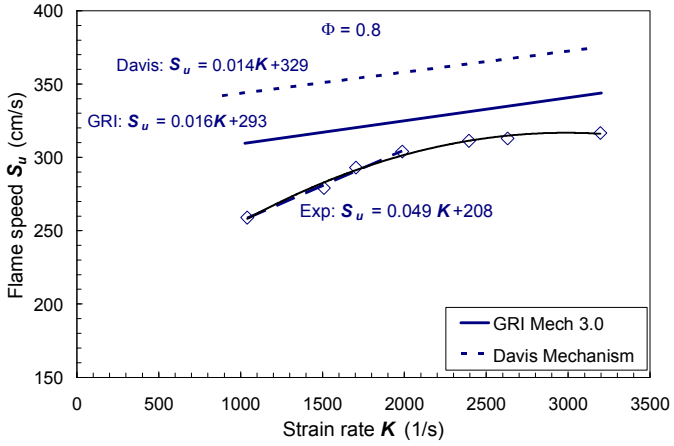

Figure 9 Strained laminar flame speeds for H_2 with N_2 diluted air (O_2:N_2 1:9) at 700 K preheat temperature; data (symbols and linear fit) and OPPDIF predictions (lines).

Also shown in Figure 9 are the predicted strain flame speeds by both models in the same strain rate range as that of measurements. The predicted strain flame speeds do not have the nonlinear variation seen in the measured flame speeds, and both models over predict the measured flame speed. The GRI Mech predictions are higher than measurements by as much as 20% at lower strains. The amount of over prediction decreases to 10% as the strain rate increases. The H_2/CO mechanism over predict the measurements by as much as 30% at lower strain rates, but the discrepancy decreases to 20% as the strain rate increases. The predicted strain sensitivities by both models are very similar, but the measured strain sensitivity is three times higher than the values predicted by the models.

Experiments were also conducted for stochiometric and rich equivalence ratios for this fuel mixture at 700 K preheat temperature. Figure 10 shows the measured strained flame speed for Φ=1.0 and 1.6. Because of the high diffusivity of the H_2, the measured flame speeds for the richer case are higher than at stoichiometric conditions. The measured flame speed increases linearly for both equivalence ratios. The predicted strained flame speeds by both models are also shown in Figure 10. For both fuel-air ratios, the models over predict the measurements, with the GRI Mech having the smaller over prediction (12% at stoichiometric condition and 10% at Φ=1.6). The Davis *et al*. H_2/CO mechanism over predicts the measurement by 18% at Φ=1 and 12% at Φ=1.6. Hence, both models over predict the measurements, and the amount of over prediction decreases as the equivalence ratio increases. For all three conditions, the GRI Mech predictions are closer to measurements.

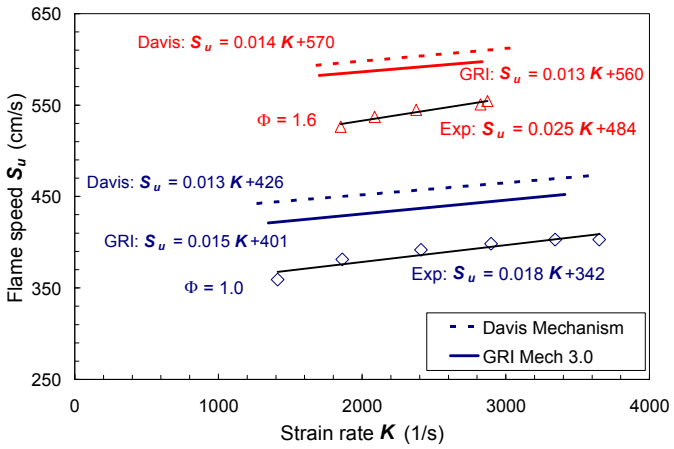

Figure 10 Strained laminar flame speeds for stoichiometric and rich H_2 with N_2 diluted air (O_2:N_2 1:9) mixtures at 700 K preheat temperature; data (symbols and linear fit) and OPPDIF predictions (lines).

It is important to note the variation of the measured strain sensitivity with equivalence ratio. The measured strain sensitivity decreases as the equivalence ratio increases from 0.8 to 1.0 (see Figure 9 and Figure 10) and then increases as the equivalence ratio increases further to 1.6 (see Figure 10). Additionally, the predicted strain sensitivities by both models do not change with equivalence ratio.

Effect of the wall

For all the strained flame speed predictions, the Chemkin opposed flow code was used with two premixed flames on either side of the stagnation plane; the simulation is adiabatic. In the experiments, however, a solid wall replaces one of the premixed jet, which makes the system nonadiabatic due to the loss of heat from the product gases to the solid wall. This could potentially reduce the unburned strained flame speed. Moreover in the opposed flame case, the radial velocity gradient at the stagnation plane is finite (due to a slip condition), while it is zero at the plug wall (due to a no slip condition) for the single jet wall case. This zero radial velocity gradient changes the strain rate distribution in the product zone, which could change the unburned flame speed. In order to investigate the effects of both heat loss and no-slip condition at the wall, a detailed numerical analysis was conducted on a wall stagnation flame configuration, and the results were compared with that of opposed flame case.

The wall stagnation flame was simulated with the Chemkin opposed flow code, but with modified boundary conditions. For the opposed flow code there are two nozzles separated by distance L. The boundary conditions at each nozzle exit are the same: $T = T_i$, $F = \rho u/2$, $G = \rho v/r = 0$, and for the species, the sum of convection and diffusion is equal to the total inflow mass flux. Here, F and G are the parameters defining axial (u) and radial (v) velocities respectively and they are function of x only. To simulate the wall stagnation flame, one of the nozzle

boundary conditions is changed as follows: the axial velocity is zero ($F=0$), the temperature is $T=T_{wall}$, the radial velocity gradient is zero ($G = 0$), and for the species the diffusive velocity is zero. All of these boundary conditions can be applied in the opposed flow code by considering the top nozzle as a solid wall and specifying $u=0$ and $T=T_{wall}$. The other two boundary conditions for the radial velocity gradient and the species are automatically satisfied. The distance between the nozzles has to be reduced from L to $L/2$. Figure 11 shows the variation of the temperature and radial velocity gradient along the axial direction for both opposed flame (OPF) and wall stagnation flame (WSF) for the same mixture, fuel-air ratio and single-jet flowrate. The distance from the nozzle exit to the stagnation plane is 0.6 cm and the axial velocity at the nozzle exit is 1.2 m/s. The temperature of the wall for the wall stagnation flame is 900 K.

For both cases, the flame is located at around 0.46 cm from the nozzle exit. The temperature for the OPF case increases and reaches a maximum (1717 K) at the stagnation plane. For the WSF case, the temperature also increases in the preheat zone, but reaches a lower maximum (1531 K) somewhere in the reaction zone and then decreases to the specified 900 K at the stagnation plane (wall). It should be noted here that due to the presence of heat loss for the WSF case, which is evident from the finite temperature gradient at the stagnation plane, the maximum temperature is much less than that of the OPF case. The radial velocity gradient, in a similar fashion to the temperature, increases and reaches maximum at the stagnation plane for the OPF case. For the WSF case, it increases and then decreases to zero at the wall in order to satisfy the no-slip condition at the stagnation plane. This indicates that there is a significant change in strain rate distribution in the product zone closer to the wall. Moreover the wall stagnation flame is slightly displaced further from the stagnation surface compared to the opposed flame case.

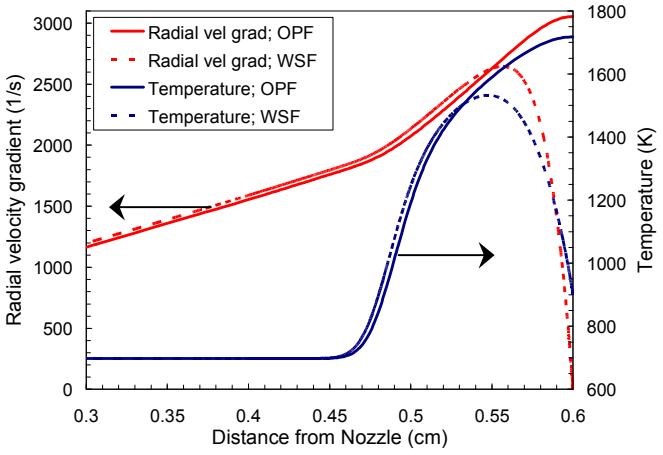

Figure 11 Numerical simulation of opposed flame (OPF) and wall stagnation flame (WSF) for H_2 with N_2 diluted air (O_2:N_2 1:9) at Φ=0.8 and 700 K preheat temperature.

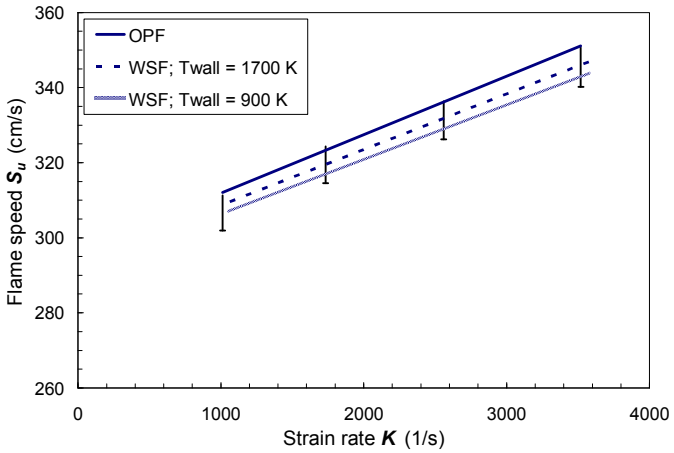

Figure 12 variation of the strained flame speed for OPF and WSF with two different wall temperatures. The fuel mixture is H_2 with N_2 diluted air (O_2:N_2 1:9) at Φ=0.8 and 700 K preheat temperature. The vertical bars indicate 3% deviation from OPF.

Numerical simulations of OPF and WSF were carried out for H_2 with N_2 diluted air (O_2:N_2 1:9) at Φ=0.8 and 700 K preheat temperature. This fuel composition is chosen for detailed investigation because it is expected to be more sensitive to heat loss for two reasons: 1) the flame is located closer to the wall (within about two flame thicknesses) compared to the other cases reported here, and 2) the temperature and velocity rise across the flame is small (i.e., a very weak flame). Figure 12 shows the strained flame speed predicted with GRI Mech over a range of strain rate for opposed flame and wall stagnation flames. For the wall stagnation flame, simulations were performed for two wall temperatures (900 and 1700 K). It is obvious that the amount of heat loss would be very small for T_{wall} = 1700 K, because the temperature at the stagnation plane for the OPF case is nearly the same value. Hence the effect of no-slip boundary condition at the wall should dominate for this simulation. For the T_{wall} = 900 K case, however, the amount of heat loss is much greater and hence the effect of both heat loss and no-slip boundary condition can be studied with this simulation.

The predicted strained flame speed increases linearly for all three cases over the range of strain rate tested. Moreover the predicted strain sensitivities are almost the same for all three cases. Comparing the strained flame speeds, the WSF predictions are always lower than the OPF predictions. The WSF predictions with T_{wall}=1700 K under predict the OPF by less than 2%. This indicates that though the temperatures at the stagnation plane are almost the same for both of these cases, the effect of zero radial velocity gradient at the wall reduces the strained flame speed. When the wall temperature is reduced further, the predicted strained flame speed decreases slightly. For the wall temperature of 900 K the predicted flame speeds under predict the OPF results by less than 3% throughout the strain rate range tested. This indicates that though the flame temperature is lower for WSF due to greater downstream heat loss from the products, this does not significantly change the

unburned strained flame speed even when the flame is located with in two flame thickness away from the wall.

CONCLUSIONS

Laminar flame speeds and strain sensitivities of mixtures of $H_2/CO/CO_2/N_2/O_2$ were measured at high preheat temperatures (700 K) and lean conditions using wall stagnation flame technique. The measurements were compared to numerical prediction based on GRI Mech 3.0 and the H_2/CO mechanism of Davis *et al*.) in order to verify their validity at gas turbine operating conditions. The calculated flame speeds from both models for 50:50 H_2:CO fuel mixtures over predict the measurements, with the H_2/CO mechanism having a greater over prediction. Moreover, the amount of over prediction by both models increases as the mixture becomes leaner. The predicted strain sensitivities are reasonably in good agreement with measurements. When this 50:50 H_2:CO fuel mixture is diluted with 40% CO_2, the discrepancies between the measurements and predictions are of the same level as those for the undiluted case, especially at very lean conditions. This indicates that the flame speed is not affected significantly by radiation absorption/emission effect of CO_2 for this mixture at highly preheated lean condition. Experiments were conducted at 5 atm pressure and room temperature for low H_2 content (5 to 20%) fuel mixtures at lean condition. While the models predict the measured flame speed and strain sensitivity well for 5 and 10% of H_2, they fail to predict the increased strain sensitivity for 20% H_2.

For pure H_2 fuel at very lean conditions, the GRI Mech results are in excellent agreement with measurements while the H_2/CO mechanism slightly over predict the measurements. The strain sensitivities are predicted reasonably well by both models. Large discrepancies between measurements and predictions were observed for pure H_2 with highly N_2 diluted air (O_2:N_2 1:9). Both mechanisms over predict the measured flame speed by as much as 20-30% at lean conditions. Moreover, the measured strain sensitivity is three times larger than the predictions at lean conditions. Though the level of flame speed over prediction decreases as equivalence ratio increases to stoichiometric and rich condition, the models fail to predict the measured strain sensitivity variation with Φ. It has also been shown that the downstream heat loss from the products to the wall and zero radial velocity gradient at wall has insignificant effect (less than 3%) on the unburned flame speed and strain sensitivity though the flame is located within two flame thickness from the stagnation plane.

In summary, leading models employed to predict syngas flame speeds and strain sensitivity are reasonably accurate for medium H_2 content fuel mixtures (with and without CO_2 dilution) and pure H_2-Air fuel mixtures at highly preheated lean conditions. But the models largely over predict the flame speed and under predict the strain sensitivity at lean condition for pure H_2 with N_2 diluted air and also they fail to predict the change in strain sensitivity with equivalence ratio.

ACKNOWLEDGEMENTS

The authors would like to acknowledge the support of GE Global Research and Development (contract DE-PS26-99FT40578) and Siemens Power Generation under a subcontract from the U.S. Department of Energy. The authors would also like to thank Prof. Hai Wang for providing the Davis H_2/CO mechanism.

REFERENCES

[1]Moliere, M. (2002). "Benefiting from the wide fuel capability of gas turbines: A review of application opportunities." *ASME Paper GT-2002-30017*.

[2]Klimstra, J (1986). "Interchangeability of Gaseous Fuels – The Importance of the Wobbe Index," *SAE Paper 861578*.

[3]Scholte, T. G., and Vaags, P. B. (1959). "Burning velocities of mixtures of hydrogen, carbon monoxide, and methane with air." *Combustion and Flame* **3**, 511-524.

[4]Günther, R., and Janisch, G. (1971). "Messwerte der Flammegeschwindigkeit von gasen und gasmischen." *Chemie-Ing-Techn.* **43**: 975-978.

[5]Strauss, W. A., and Edse, R. (1958). "Burning velocity measurements by the constant-pressure bomb method." *Proceedings of the Combustion Institute* **7**: 377-385.

[6]Yumlu, V. S. (1967). "Prediction of burning velocities of carbon monoxide-hydrogen-air flames." *Combustion and Flame* **11**: 190-194.

[7]Vagelopoulos, C. M., and Egolfopoulos, F. N. (1994). "Laminar flame speeds and extinction strain rates of mixtures of carbon monoxide with hydrogen, methane, and air." *Proceedings of the Combustion Institute* **25**: 1317-1323.

[8]McLean, I. C., Smith, D. B., and Taylor, S. C. (1994). "The use of carbon monoxide/hydrogen burning velocities to examine the rate of the CO + OH reaction." *Proceedings of the Combustion Institute* **25**: 749-757.

[9]Brown, M. J., McLean, I. C., Smith, D. B., and Taylor, S. C. (1996). "Markstein lengths of CO/H_2/air flames, using expanding spherical flames." *Proceedings of the Combustion Institute* **26**: 875-881.

[10]Hassan, M. I., Aung, K. T., and Faeth, G. M. (1996). "Markstein numbers and unstretched laminar burning velocities of wet carbon monoxide flames." *AIAA 96-0912*, *34th Aerospace Sciences Meeting & Exhibit, Reno, NV*.

[11]Hassan, M. I., Aung, K. T., and Faeth, G. M. (1997). "Properties of laminar premixed CO/H_2/air flames at various pressures." *Journal of Propulsion and Power* **13**(2): 239-245.

[12]Ren, J.-Y., Qin, W., Egolfopoulos, F. N., Mak, H., and Tsotsis, T. T. (2001). "Methane reforming and its potential effect on the efficiency and pollutant emissions of lean methane-air combustion." *Chemical Engineering Science* **56**: 1541-1549.

[13]Qin, W., Egolfopoulos, F. N., and Tsotsis, T. T. (2001). "Fundamental and environmental aspects of landfill gas utilization for power generation." *Chemical Engineering Journal* **82**: 157-172.

[14] Natarajan, J., Nandula, S., Lieuwen, T., and Seitzman, J. (2005). "Laminar Flame Speeds of Synthetic Gas Fuel Mixtures." *ASME Paper GT-2005-68917*.

[15] Wu, C. K., and Law, C. K. (1984). "On the determination of laminar flame speeds from stretched flames." *Proceedings of the Combustion Institute* **20**: 1941-1949.

[16] Vagelopoulos, C. M., Egolfopoulos, F. N., and Law, C. K. (1994). "Further considerations on the determination of laminar flame speeds with the counterflow twin-flame technique." *Proceedings of the Combustion Institute* **25**: 1341-1347.

[17] Egolfopoulos, F. N., Zhang, H., and Zhang, Z. (1997). "Wall effects on the propagation and extinction of steady, strained, laminar premixed flames." *Combustion and Flame* **109**, 237-252.

[18] Andac, M. G., Egolfopoulos, F. N., and Campbell, C. S. (2002). "Premixed flame extinction by inert particles in normal and micro-gravity." *Combustion and Flame* **129**, 179-191.

[19] Smith, G. P., Golden, D. M., Frenklach, M., Moriarty, N. W., Eiteneer, B., Goldenberg, M., Bowman, C. T., Hanson, R. K., Song, S., Jr Gardiner, W. C., Lissianski, V. V., and Qin, Z. http://www.me.berkeley.edu/gri_mech/

[20] Davis, S. G., Joshi, A. V., Wang, H., and Egolfopoulos, F. N. (2004). "An optimized kinetic model of H_2/CO combustion" *Proceedings of the Combustion Institute* **30**. 1283-1292.